Egyptian Journal of Chemistry

http://ejchem.journals.ekb.eg/

Flammability Properties of Polyvinyl Alcohol Containing New Flame Retardant System

Ghada Makhlouf [a,*], Aksam Abdelkhalik [a, *], Randa Nasr [b], M. A. Hassan [c]

[a] *Fire and explosion protection laboratory,* [b] *Reference material laboratory, National Institute of Standards, El-Sadat street, El-Haram, El-Giza, P.O.Box 136, Code 12211, Egypt*
[c] *Saudi Standards, Metrology and Quality Organization, P.O.Box 3437 Riyadh 11471 kingdom of Saudi Arabia*

Abstract

In this work, graphite (G), ammonium iron (II) sulfate (AFS) and aluminium nitrate were added to polyvinyl alcohol (PVA) at 25% loading level to improve its flame retardancy. In addition, PVA/(G+AFS+AN) composite was prepared. The flammability and smoke density of PVA composites were evaluated by UL94 flame chamber, limiting oxygen index (LOI) and smoke density chamber. Vertical flame spread test (UL94V) indicated that PVA composites achieved V0 class in PVA/(G+AFS+AN)and PVA/AFS samples. Horizontal burning rate (UL94H) data showed that PVA composites achieved H0 class. LOI of PVA was enhanced from 19.1% to 21.3%, 25.2%, 26.1% and 27.2% in PVA/G, PVA/AN, PVA/AFS and PVA/(G+AFS+AN)composites, respectively. The maximum specific optical density (Ds_{max}) of PVA was decreased in all PVA composites due to the formation of protective char layer on polymer surface. The maximum reduction in Ds_{max} value of PVA was 64% and it was observed in PVA/(G+AFS+AN). XRD analysis of char residue after smoke density test of PVA/(G+AFS+AN) indicated the presence of coquimbite phase, graphite and magnetite in the char residue. Thermogravimetric analysis (TGA) data of PVA and PVA/(G+AFS+AN) composite showed that the new flame-retardant system improved the thermal stability of neat polymer and the temperatures at which 50% ($T_{50\%}$) weight loss takes place were greatly enhanced. In addition, the char residue at 750 ℃ was increased.

Keywords: PVA; graphite; smoke density; ammonium iron (II) sulfate; aluminium nitrate

1. Introduction

PVA is widely used in many applications because it is easy to process, has excellent chemical resistance, water soluble and biodegradable polymer [1- 4]. PVA can be used in the manufacturing of fibers, proton exchange membranes, clothes, packing materials, adhesives, films and artificial biomedical devices [5-14]. Unfortunately, PVA is highly flammable material with LOI (19 ±0.1%) and fails to achieve class in UL94V test [13-19]. Therefore, much research work was directed to improve the flame retardancy of PVA. To attain excellent flame retardancy, PVA was mixed with inorganic additives like montmorillonite (MMT), α-zirconium phosphate (ZrP) and hectorite (HC). Lu et al. [17, 19] presented

that addition of 8 phr of ZrP, MMT and HC to PVA were able to decrease the first peak of heat release rate (pHRR1) rate in Microscale Combustion Calorimeter (MCC) test. The reductions in pHRR1 showed the following order: HC < MMT < ZrP [17]. Also, the authors published that addition of ethylamine modified zirconium phosphate (ZrP-EA) at 8 phr to PVA reduced pHRR1 and total heat release (THR) of PVA by 42% and 16.6%, respectively [19]. Liu et al. [2] studied the effect of inserting MMT to PVA(85%)/APP(15%) system. The authors stated that LOI value of PVA(85%)/APP(15%) increased from 27.9% to 30.8% in PVA(85%)/APP(14.3%) /MMT (0.7%) composite. Zhao et al. [20] studied the effect of

_____

adding different kinds of layered double hydroxides (LDH) to PVA(85%)/APP (15%) system. They reported that PVA(85%)/APP (15%) had LOI value 27.5% and failed to achieve class in UL94V test. In contrast, PVA(85%)/APP (14.7%)/Zn-Al –LDH (0.3%), PVA(85%)/APP (14.7%)/Ni-Fe –LDH (0.3%) and PVA(85%)/APP (14.7%)/Zn-Fe –LDH (0.3%) showed LOI values 30.6%, 33.6% and 32.8%, respectively and these composites were able to achieve V0 in UL94V test. Increasing the wt.% of LDH to be more than 0.3% led to decreasing in LOI values [20]. Luo et al. [21] applied (α-ZrP) and APP to improve the flame retardancy of PVA aerogels. The authors showed that the best flame-retardancy synergism was obtained between 13%APP and 2% α-ZrP where PVA85%/APP13%/2%ZrP composite had LOI result (43.1%) while PVA85%/APP15% composite showed LOI value (37.5%). As well cone calorimeter data lay out that adding APP15% and APP13%/2%ZrP to PVA decreased its pHRR by 68.8% and 82.5% respectively. Cai et al. [22] reported that addition of pseudo-boehmite nanorods to PVA improved the LOI value. The Δ LOI value (LOI of the composite – LOI of PVA) reached 10.5% at loading level 37.5 wt% of pseudo-boehmite nanorods. Haung et al. [23] prepared nanocomposites based on PVA and graphene nanosheets and studied the effect of graphene on the flammability properties of PVA. The interesting result in this work was that addition of 5 wt% graphene to PVA increased time to ignition in cone calorimeter test from 18 s in PVA to 45 s in PVA/5 wt% graphene nanocomposite. Moreover, pHRR and THR of PVA was decreased by 64.3% and 34.4%, respectively [23]. Wang et al. [24] used nanosheet from hexagonal boron nitride@$ZnFe_2O_4$ (h-BN@$ZnFe_2O_4$) hybrid to enhance the flame retardancy of PVA. Cone calorimeter data indicated that pHRR of PVA containing h-BN@$ZnFe_2O_4$ (7 wt%) was lower than neat polymer by 59%. In addition, PVA nanocomposites produced lower concentrations from CO, CO_2 and hydrocarbon gases relative to pure PVA. Xu et al. [4] prepared PVA foam beads by super critical CO_2 foaming and pelletizing. The authors used a solution of potassium silicate (KSi) to coat the surfaces of PVA beads. The flammability tests indicated that PVA/28.6 wt% KSi sample attained V0 and 33.7% in UL94 and LOI tests, respectively.

Graphite is one of carbon base materials which are including also carbon black, graphene, carbon nano tubes and fullerene. G consists of accumulated graphene nano sheets where the carbon atoms inside sheets form hexagonal cells with covalent bonds and the carbon layers are linked by van der Waals forces. Although, G is naturally abundant and cost-effective compound compared with the other carbon based materials, it is scarce to be used as flame retardant material. This is referred to that carbon flakes in graphite are closely stacked which restricts the penetration of polymer chains into the openings of the graphite sheets [25]. Abdelkhalik et al. [26] dispersed G flakes in melamine salt of pentaerythritol phosphate (MPP) and used the new mixture (MPP- G) to improve the flame retardancy of natural rubber. The authors stated that addition of 40 phr G to natural rubber reduced its pHRR by 39.1% while inserting 40 phr (MPP- G) decreased the pHRR by 64.3%.

The aims behind this work were mixing G, AFS and AN with PVA to improve its flame retardancy. Moreover, the synergistic effect between (G + AFS + AN) on the flammability properties of PVA was studied. The smoke density, vertical flame spread , horizontal rate of burning, LOI and thermal stability properties of the prepared composites were studied by smoke density chamber, UL94V, UL94H, LOI and TGA instruments.

2. Experimental

2.1. Materials
Graphite powder with carbon content 98% was purchased from LOBA Chemie Company, India. Aluminium nitrate, Al $(NO_3)_3.9H_2O$, with purity 98% and Ammonium iron (II) sulfate, $(NH_4)_2SO_4.FeSO_4.6H_2O$, with purity 99% were obtained from WINLAB Company, UK. Polyvinyl alcohol with molecular weight 115000 and degree of polymerization 1700 – 1800 was obtained from Oxford Lab Chem, India. Deionized water was obtained using purite select fusion unit, UK.

2.2. Preparation of PVA composites
To prepare PVA/G composite, 75 g of PVA were dissolved in deionized water (1 L) by heating at 80 °C using hot plate with mechanical stirrer at 800 rpm for 1 h. After dissolving PVA in water, 25 g of G were added to PVA solution and stirred at 800 rpm for 30 min. Then, PVA/G composite was poured into glass plates to cool to room temperature. Finally, the sample in glass plate was placed in an oven at 65 ℃ for 96 h to remove the excess water. The other PVA composites which contained AFS, AN, (AFS + AN) and (G + AN + AFS) were prepared by the same procedure. During preparation of PVA/(G+AN+AFS) composite, G was physically mixed with AN and AFS using spatula, then the mixture was added to PVA solution. Table 1 shows the formulations of PVA composites.

_____

Table 1:Formulations of PVA composites.

Sample code	PVA (g/ L_{water})	G (g/ L_{water})	AN (g/ L_{water})	AFS (g/ L_{water})
PVA	100	0	0	0
PVA/G	75	25	0	0
PVA/AN	75	0	25	0
PVA/AFS	75	0	0	25
PVA/(AFS+ AN)	75	0	12.5	12.5
PVA/(G + AFS + AN)	75	2.2	11.4	11.4

2. Measurements

X-ray diffractograms were taken using Empyrean diffractometer from Panalytical Co., the Netherlands, with CuKα radiation, 1.54 Å, 40 kV and 40 mA. The range of diffraction angle was $2\theta = 4°$ to $100°$ and the scanning rate was $0.013°$ per second. Scanning Electron microscope (SEM) images were taken by Quanta 250 FEG (Field Emission Gun) produced by FEI Company, the Netherlands. The SEM was linked with EDXS unit which has an accelerating voltage of 30 kV. Thermal analysis data were collected by thermogravimetric analyser (TGA50) which was obtained from Shimadzu Company, Japan. Samples were positioned in platinum crucible and samples weights were about $6 – 6.5$ mg. The measurements were carried out under nitrogen atmosphere with flow rate 30 mL/min, the heating rate was 10 ℃/min and the temperature increased gradually from room temperature to 750 ℃. LOI test was carried out at Table 2

Results of LOI, UL94H and UL94V tests for PVA and its composites.

room temperature using oxygen index instrument which was purchased from Fire Testing Technology Company, UK. The measurements were executed according to standard test method ISO 4589. Vertical and horizontal burning rate measurements were performed using UL94 chamber according to ASTM D 3801 and ASTM D 635. The rate of burning was calculated as the average of five test samples. Maximum specific optical density (Ds_{max}) was determined by smoke density chamber, supplied by Fire Testing Technology Company, UK, according ISO 5659 part 2 at horizontal heat flux 25 kW/m². The tests were carried out under flaming conditions. The data reported are the average of three tested samples.

4. Results and discussion

4.1. Flammability of PVA and its composites

4.1.1. LOI data

Sample	LOI % [a] (± 0.3)	[b]Δ LOI %	UL94H (mm/min) [a](± 1.2)	UL94V
PVA	19.1	-	40.6	No rating
PVA/G	21.3	2.2	H0	No rating
PVA/AN	25.2	6.1	H0	No rating
PVA/AFS	26.1	7	H0	V0
PVA/(AFS + AN)	25.8	6.7	H0	No rating
PVA/(G+AFS+AN)	27.2	8.1	H0	V0

a: is the expanded uncertainty. b: (LOI of composite – LOI of PVA).

The flammability properties of PVA and its composites were evaluated by LOI test. The data in Table 2 shows that LOI of PVA was 19.1%. Addition of G, AFS, AN, (AFS+AN) and (G+AFS+AN) to PVA improved its LOI value. ΔLOI is the difference between LOI value of PVA composite and LOI of pure PVA. It is clearly seen in Table 2 that LOI of PVA was increased by 2.2%, 7%, 6.1%, 6.7% and 8.1% in PVA/G, PVA/AFS, PVA/AN, PVA/(AFS + AN) and PVA/(G+AFS+AN), respectively. The maximum improvement was observed in PVA/(G+AFS+AN) composite which confirmed the

synergistic effect between G/AFS/AN to enhance the flame retardancy of PVA. This may be referred to formation of char layer which containing polyaromatic structure, Al_2O_3, Fe_2O_3 and graphite that are chemically interacted and prevented the polymer from the effect of flame [27-37].

4.1.2. Horizontal burning rate (UL94H) and vertical flame spread (UL94V) results

Horizontal burning rate test presented that PVA burnt completely and its rate of burning was 40.6 mm/min, see Table 2. Moreover, PVA failed to achieve class in

_____

vertical flame spread test. This indicates that PVA is highly flammable material at ambient conditions. Addition of 25 wt% G to PVA decreased its rate of burning to 36 mm/min (achieved H0 class) but the samples failed to achieve class in UL94V test. PVA/AFS, PVA/AN, PVA/(AFS+AN) and PVA/(G+AFS+AN) samples achieved H0 class in UL94H test. Moreover, PVA/AFS and PVA/(G+AFS+AN) composites achieved V0 class in UL94V test. According to LOI, UL94H and UL94V data, PVA/AFS and PVA/(G+AFS+AN) presented the best flame retardancy effect on PVA.
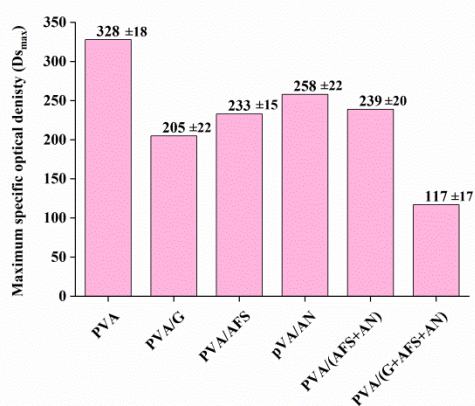
4.1.3. Smoke density data

Fig. 1. Maximum specific optical density (Ds$_{max}$) of PVA and its composites.

Smoke density data of PVA and its composites are presented in Fig. 1. Pure polymer has maximum specific optical density (Ds$_{max}$) 328. This value was decreased by adding the selected fillers to PVA. The amount of reductions in Ds$_{max}$ value of PVA were 37.5%, 28.9%, 21.3%, 27.1% and 64.3% for PVA/G, PVA/AFS, PVA/AN, PVA/(AN+AFS) and PVA/(G+AFS+AN), respectively. The composite PVA/(G+AFS+AN) showed the maximum reduction in Ds$_{max}$. This reduction in smoke density is referred to the formation of insulating char layer on PVA surface which was able to keep the polymer from the effect of heat [36, 37].

4.1.4. XRD, SEM and EDXS analysis of char residue and flame retardant mechanism

The char residue of PVA/(G+AFS+AN) composite after smoke density test was analysed by XRD, SEM and EDXS. XRD curve in Fig. 2 shows that, a new phase coquimbite (Al$_{1.80}$Fe$_{6.20}$S$_{12}$O$_{84}$, card No. 96-900-0207) was formed with typical peaks at 10.66°, 17.88° and 24.93°, respectively [34]. In addition to

coquimbite phase, the main peaks of G and magnetite were appeared [26, 35]. SEM image, Fig. 3, for char residue indicated the formation of coherent insulating char layer during PVA/(G+AFS+AN) combustion. EDXS analysis in Fig. 3 presented that C, O, Al, Fe, N and S were the main components of char layer.

The mechanism of PVA/(G+AFS+AN) composite flame retardation can be described as follow: during PVA composite combustion, it decomposed to give CO, CO$_2$ and H$_2$O in the gas phase [30-32]. In addition, AFS and AN degraded to produce SO$_2$, NO and NO$_2$ gases [28, 29]. On the other hand, XRD, SEM image and EDXS analysis indicated that in the condensed phase Al, Fe, C, O, N, and S elements were interacted during combustion to form char layer which acted as physical barrier on polymer surface. This physical barrier protected the polymer matrix from the effect of heat and flame. Moreover, it reduced the amounts of flammable volatile organic compounds which were leaving polymer matrix to combustion zone [26, 36, 37]. Also, the insulating char layer succeeded in reducing the smoke production of PVA composites relative to pure polymer.

4.2. TGA data of G, AFS, AN, PVA and its composites

TGA data of G, AFS, AN, (G+AFS+AN), PVA and PVA/(G+AFS+AN) composite are presented in Table 3 and Fig. 4(a,b,c,d). G sample is characterised by high thermal stability, it did not show weight loss till 687 ℃ and its total weight loss at 750 ℃ is 1.2%. This weight loss is referred to moisture loss and separation of adsorbed oxygen atoms [21]. AFS decomposes through dehydration, deammonisation and desulfonation [28]. These reactions occur within six decomposition steps as it is clear in TGA and Dr.TGA curves (Fig. 4(a,b)). Dehydration takes place in the temperature range 60 ℃ – 167 ℃. The Dr.TGA curve shows that the temperature at which maximum decomposition of AFS occurs (T_{max}) lies within this decomposition step where T_{max} is 95 ℃. The increase in temperature leads to phase transition (changing from amorphous state after releasing water molecules to crystalline state) nearly at 200 ℃ [28]. The phase transition is accompanied by deammonisation which involves decomposition of
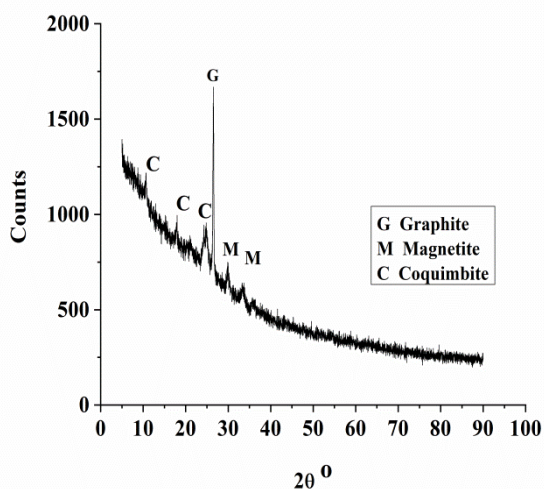
Fig. 2. XRD analysis of char residue of PVA/(G+AFS+AN) composite after smoke density test.

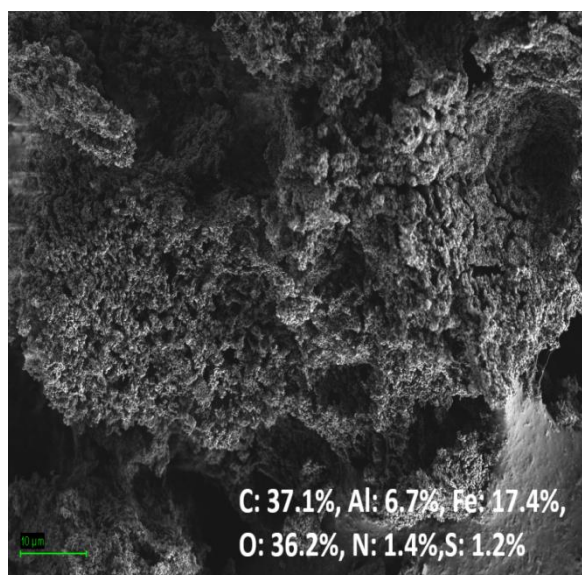C: 37.1%, Al: 6.7%, Fe: 17.4%, O: 36.2%, N: 1.4%,S: 1.2%

Fig. 3. SEM image and EDXS analysis (elements are in wt%) of char residue of PVA/(G+AFS+AN) composite after smoke density test.

ammonium sulfate [28]. After losing ammonia, the salt becomes mixture of ferrous sulphate and ferric sulphate. Within the temperature range 450 ℃ – 660 ℃, this mixture decomposes to form α-Fe_2O_3 [28]. According to the data in Table 3, AFS left 19.7% as a char residue at 750 ℃. The thermal decomposition of AN takes place through condensation of two moles from the initial monomer (AN) [29]. Then, the resulting product $Al_2(NO_3)_6 13H_2O$ loses HNO_3 + H_2O subsequently N_2O_3 and O_2 which are resulting from N_2O_5 decomposition. During this process oxynitrate

compound $Al_2O_2(NO_3)_2$ is formed and it is transformed to Al_2O_3 [29]. AN sample started to lose adsorbed moisture and crystallization water at 45 ℃ and lost 4.9% of its weight in the temperature range 45 ℃ – 75 ℃. The second decomposition stage (between 78 ℃ – 160 ℃) shows the greatest weight loss (62.6%) in AN curve. This weight loss is referred to releasing water vapour and nitric acid [29]. Fig. 4b displays that T_{max} of AN lies within this decomposition step where T_{max} value is 129 ℃.The next weight loss is 16.1% and it is found in the temperature range 160 ℃ – 400 ℃. During this stage N_2O_3 and O_2 are released besides traces of HNO_3. In the temperature range 400 ℃ – 750 ℃ (Fig. 4a), the residual char of sample is thermally stable due to formation of Al_2O_3 and the weight loss is only 1.6% [29]. AN sample left lower amount from char residue (14.4%) at 750 ℃ compared with G and AFS.

TGA of PVA and PVA/(G+AFS+AN) composite, Fig. 4c, shows a slight weight loss in the temperature range 60 ℃ – 160 ℃ which is referred to losing of adsorbed water. It was reported that PVA decomposes through two steps where the first step involves weight loss due to dehydration and depolymerization of PVA followed by polyene formation. The second decomposition step includes pyrolysis of polyene formed during the first step, and it accompanied by producing certain volatile organic compounds [30-32]. PVA attains $T_{50\%}$ and $T_{80\%}$ at 268 ℃ and 417 ℃, and leaves 2.3% as char residue at 750 ℃. Fig. 4d presents that T_{max} of PVA locates at 266 ℃. PVA/(G+AFS+AN) composite decomposed through two main steps like PVA and the addition of (G+AFS+AN) to PVA improves $T_{50\%}$ and $T_{80\%}$ values (see Table 3). $T_{50\%}$ and $T_{80\%}$ of PVA were increased by 87 ℃ and 247 ℃ in PVA/(G+AFS+AN) composite. Also, Fig. 4d indicates that T_{max} of PVA/(G+AFS+AN) is 285 ℃ and it is higher than T_{max} of pure PVA (266 ℃). This great improvement in $T_{50\%}$ and $T_{80\%}$ is referred to formation of insulating char layer which protected the polymer from the effect of heat. The char layer is expected to contain Al_2O_3, graphite and Fe_2O_3. The residual char at 750 ℃ was enhanced from 2.3% in pure polymer to 19% in PVA/(G+AFS+AN) sample. Moreover, the theoretical char residue is 7.8% while the practical value is 19%. This confirms the synergistic effect between G, AFS and AN to enhance formation of char layer on PVA surface which acts as a physical barrier and protect the polymer from the effect of heat at high temperature [36].

Table 3
TGA results of G, AFS, AN, PAV and PVA/(G+AFS+AN) composite.

Sample code	^aT_i ℃	$^bT_{50\%}$ ℃	$^cT_{80\%}$ ℃	^{d} Char at 750 ℃ (%)	^{e} Char at 750 ℃ (%)
G	687	-	-	98.8	-
AFS	60	433	714	19.7	-
AN	45	136	277	14.4	-
PVA	60	268	417	2.3	-
PVA/(G+ AFS+AN)	59	355	664	19	7.8

a:temperature at which material started decomposition.
b : temperature at which 50% weight loss takes place.
c : temperature at which 80% weight loss takes place.
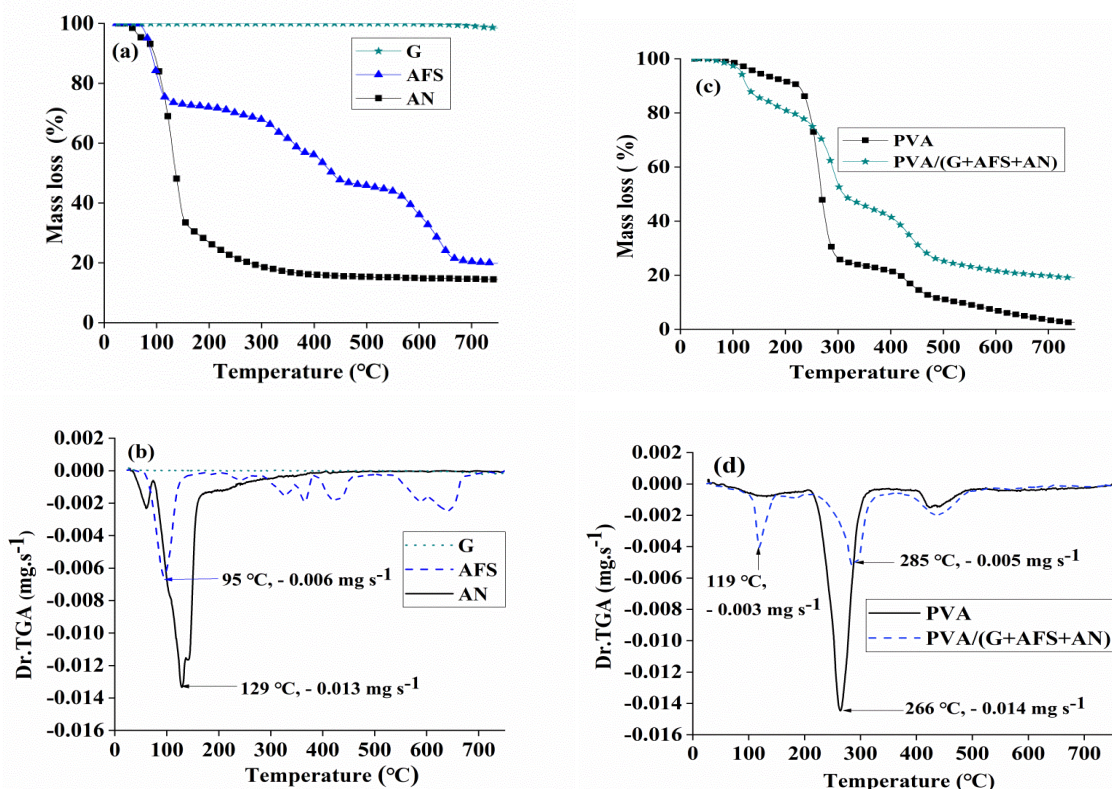d: practical char residue.
e: theoritical char residue.

Fig. 4. (a) TGA of G, AN, AFS; (b) Dr.TGA of G, AN, AFS; (c) TGA of PVA and PVA/(G+AFS+AN)
composite; (d) Dr.TGA of PVA and PVA/(G+AFS+AN) composite.

5. Conclusions

1. In this study G, AFS, AN, (AFS + AN) and (G + AFS + AN) were added to PVA. The flammability properties of PVA composites were studied and compared.
2. Horizontal burning rate test showed that all composites achieved H0 class. The flame did not propagate in PVA/AFS, PVA/AN, PVA/(AFS + AN) and PVA/(G + AFS + AN) samples.
3. Vertical flame spread test indicated that PVA/AFS and PVA/(G+AFS+AN) samples achieved V0 class. In contrast, PVA/AN, PVA/G, PVA/(AN+AFS) samples failed to achieve class in UL94V test.
4. LOI value of PVA was improved and it increased by 2.2%, 7%, 6.1%, 6.7% and 8.1% in PVA/G, PVA/AFS, PVA/AN, PVA/(AFS + AN) and PVA/(G+AFS+AN), respectively.
5. The maximum value for specific optical density, Ds_{max}, of PVA was reduced by

37.5%, 28.9%, 21.3%, 27.1%, 64.3% for PVA/G, PVA/AFS, PVA/AN, PVA/(AN + AFS) and PVA/(G+AFS+AN), respectively.

6. PVA/(G+AFS+AN) composite showed the highest LOI value (27.2%) and the lowest Ds_{max} (117). This confirmed the synergistic effect between the components (G/AFS/AN) to improve the flame retardancy of PVA.

7. XRD analysis of char residue of PVA/(G+AFS+AN) composite after smoke density test showed the formation of coquimbite phase ($Al_{1.80}Fe_{6.20}S_{12}O_{84}$). Besides, G and magnetite were also found in the char residue. This indicated that the components (G/AFS/AN) retard the flame in the condensed phase by forming char layer (containing Al, Fe, O, C, S and N atoms) on polymer surface to protect it from the effect of heat and flame.

8. TGA data indicated that addition of (G+AFS+AN) to PVA enhanced its thermal stability at high temperatures and increased the formation of char residue at 750 °C.

6. Conflicts of interest
There are no conflicts to declare.

References
[1] Xu X., Uddin A. J., Aoki K., Gotoh Y., Saito T., Yumura M., Fabrication of high strength PVA/SWCNT composite fibers by gel spinning. *Carbon,* 48(7), 1977-1984(2010).
[2] Lin J. S., Liu Y., Wang D. Y., Qin Q., Wang Y. Z., Poly(vinyl alcohol)/ammonium polyphosphate systems improved simultaneously both fire retardancy and mechanical properties by montmorillonite. *ACS Ind Eng Chem Res*, 50(17), 9998-10005(2011).
[3] Xu L., Lei C., Xu R., Zhang X., Zhang F., Hybridization of α-zirconium phosphate with hexachlorocyclotriphosphazene and its application in the flame retardant poly(vinyl alcohol) composites. *Polym Degrad Stab,* 133, 378-388(2016).
[4] Xu D., Liu P., Wang Q., Interfacial flame retardance of Poly(vinyl alcohol) bead foams through surface plasticizing and microwave selective sintering. *Appl Surf Sci,* 551, 149416(2021).
[5] Lin M., Yang Y., Xi P., Chen S., Microencapsulation of water- soluble flame retardant containing organophosphorus and its application on fabric. *J Appl Polym Sci,* 102(5), 4915-4920(2006).
[6] Mercader C., Denis-Lutard V., Jestin S., Maugey M., Derre A., Zakri C., Poulin P., Scalable process for the spinning of PVA–carbon nanotube composite fibers. *J Appl Polym Sci,* 125(51), 191-196(2012).
[7] Lee S. C., Shin K. L., Oh B. H., Cyclic pull-out test of single PVA fibers in cementitious matrix. *J Compos Mater,* 45(26), 2765-2772(2011).
[8] Kaboorani A., Riedl B., Improving performance of polyvinyl acetate (PVA) as a binder for wood by combination with melamine based adhesives. *Int J Adhes,* 31(7), 605-611(2011).
[9] Mohsen-Nia M., Modarress H., Viscometric study of aqueous poly(vinyl alcohol) (PVA) solutions as a binder in adhesive formulations. *J Adhes Sci Technol,* 20(12), 1273-1280(2006).
[10] Banerjee D., Jha A., Chattopadhyay K. K., Synthesis and characterization of water soluble functionalized amorphous carbon nanotube-poly(vinyl alcohol) composite. *Macromol Res,* 20, 1021-1028(2012).
[11] Mallakpour S., Madani M., Transparent and thermally stable improved poly (vinyl alcohol)/Cloisite Na^+/ZnO hybrid nanocomposite films: Fabrication, morphology and surface properties. *Prog Org Coat,* 74(3), 520-525(2012).
[12] Pourjafar S., Rahimpour A., Jahanshahi M. J., Synthesis and characterization of PVA/PES thin film composite nanofiltration membrane modified with TiO_2 nanoparticles for better performance and surface properties. *Ind Eng Chem Res,* 18(4), 1398-1405(2012).
[13] Serbezeanu D., Vlad-Bubulac T., Hamciuc C., Hamciuc E., Grădinaru L., Lisa G., Anghel I., Ioana-Emilia Şofran L., Mocioi L., Enache A,Poly (vinyl alcohol)-oligophosphonate eco-friendly composites with improved reaction-to-fire properties. *Compos Commun,* 22, 100505(2020).
[14] Liu P., Chen W., Liu Y., Bai S., Wang Q., Thermal melt processing to prepare halogen-free flame retardant poly(vinyl alcohol). *Polym Degrad Stab,* 109, 261-269(2014).
[15] Zhang H., Zhang J, The preparation of novel polyvinyl alcohol (PVA)-based nanoparticle/carbon nanotubes (PNP/CNTs) aerogel for solvents adsorption application. *J Colloid Interface Sci,* 569, 254-266(2020).
[16] Ye T., Zou Y., Xu W., Zhan T., Sun J., Xia Y., Zhang X., Yang D., Poorly-crystallized poly(vinyl alcohol)/carrageenan matrix: Highly ionic conductive and flame-retardant gel polymer electrolytes for safe and flexible solid-state supercapacitors. *J Power Sources,* 475, 228688 (2020).
[17] Lu H., Wilkie C., Ding M., Song L., Flammability performance of poly(vinyl alcohol) nanocomposites with zirconium

phosphate and layered silicates. *Polym Degrad Stab,* 96(7), 1219-1224(2011).

[18] Yang Z., Li H., Niu G, Wang J., Zhu D., Poly(vinylalcohol)/chitosan-based high-strength, fire-retardant and smoke-suppressant composite aerogels incorporating aluminum species via freeze drying. Compos B Eng, 219, 108919(2021).

[19] Lu H., Wilkie C., Ding M., Song L., Thermal properties and flammability performance of poly (vinyl alcohol)/α-zirconium phosphate nanocomposites. *Polym Degrad Stab*, 96(5), 885-891(2011).

[20] Zhao C., Liu Y., Wang D. Y., Wang D. L., Wang Y. Z., Synergistic effect of ammonium polyphosphate and layered double hydroxide on flame retardant properties of poly(vinyl alcohol). Polym Degrad Stab, 93(7), 1323-1331(2008).

[21] Luo Y., Xie D., Chen Y., Han T., Chen R., Sheng X., Mei Y., Synergistic effect of ammonium polyphosphate and α-zirconium phosphate in flame-retardant poly(vinyl alcohol) aerogels. *Polym Degrad Stab*, 170, 109019(2019).

[22] Cai Y., Zhao M., Wang H., Li Y., Zhao Z., Synthesis and properties of flame-retardant poly(vinyl alcohol)/ pseudo-boehmite nanocomposites with high transparency and enhanced refractive index. *Polym Degrad Stab,* 99, 53-60(2014).

[23] Huang G., Gao J., Wang X., Lian H., Ge C., How can graphene reduce the flammability of polymer nanocomposites?. *Mater Lett,* 66(1), 187-189(2012).

[24] Wang X., Yin Y., Li M., Hu Y., Hexagonal boron Nitride@ZnFe2O4 hybrid nanosheet: An ecofriendly flame retardant for polyvinyl alcohol. *J Solid State Chem,* 287, 121366 (2020).

[25] Wang X., Kalali E., Wan J., Wang D., Carbon-family materials for flame retardant polymeric materials. *Prog Polym Sci,* 69, 22-46(2017).

[26] Abdelkhalik A., Makhlouf G., Abdel- Hakim A., Fire behavior of natural rubber filled with intumescent flame retardant containing graphite. *J Vinyl Addit Technol,* 26(2), 155-164(2020).

[27] Zhang G., Wen M., Wang S., Chen J., Wang J., Insights into thermal reduction of the oxidized graphite from the electro-oxidation processing of nuclear graphite matrix. *RSC Adv,* 8, 567-579(2018).

[28] https://shodhganga.inflibnet.ac.in/bitstream/10603/143376/9/09_chapter%204.pdf. Accessed April, 2020. Chapter 4.Thermal decomposition of double sulfates.

[29] Melnikov P., Nascimento V. A., Arkhangelsky I. V., Consolo L. Z., Thermal decomposition mechanism of aluminum nitrate octahydrate and characterization of intermediate products by the technique of computerized modelling. *J Therm Anal Calorim,* 111, 543-548(2013).

[30] Gaikwad K. K., Lee J. Y., Lee Y. S., Development of polyvinyl alcohol and apple pomace bio-composite film with antioxidant properties for active food packaging application. *J Food Sci Technol,* 53(3), 1608-1619(2015).

[31] Dong S., Wu F., Chen L., Wang Y., Chen S., Preparation and characterization of Poly(vinyl alcohol)/graphene nanocomposite with enhanced thermal stability using PEtVIm-Br as stabilizer and compatibilizer. *Polym Degrad Stab,* 131, 42-52(2016).

[32] Zaikov G. E., Lomakin S. M., Flame retardants: poly(vinyl alcohol) and silicon compounds. In: Pritchard, G., (eds.) Plastic Additives. Polymer Science and Technology Series, 1998; pp. 55-56. Spronger, Dordrecht.

[33] Molyneux S. A., Stec A. A., Hull T. R., The correlation between carbon monoxide and hydrogen cyanide in fire effluents of flame retarded polymers. Fire safety science-proceedings of the eleventh international symposium,389-403(2014). 10.3801/IAFSS.FSS.11-389.

[34] Frost R., Gobac Ž., López A., Xi Y., Scholz R., Lana C., Lima R., Characterization of the sulphate mineral coquimbite, a secondary iron sulphate from Javier Ortega mine, Lucanas Province, Peru – Using infrared, Raman spectroscopy and thermogravimetry. *J Mol Struct,* 1063, 215-258(2014).

[35] Mahadevan S., Gnanaprakash G., Philip J., Rao B., Jayakumar T.,X-ray diffraction-based characterization of magnetite nanoparticles in presence of goethite and correlation with magnetic properties. *Physica E Low Dimens Syst Nanostruct,* 39(1), 20-25(2007).

[36] Abdelkhalik A., Makhlouf G., Hassan M., Manufacturing, thermal stability, and flammability properties of polypropylene containing new single molecule intumescent flame retardant. *Polym Adv Technol,* 30(6), 1403-1414 (2019).

[37] Makhlouf G., Abdelkhalik A., Hassan M., Combustion toxicity of polypropylene containing melamine salt of pentaerythritol phosphate with high efficiency and stable flame retardancy performance. *Process Saf Environ Prot,* 138, 300-311(2020).